Journal of Materials Chemistry C

Accepted Manuscript

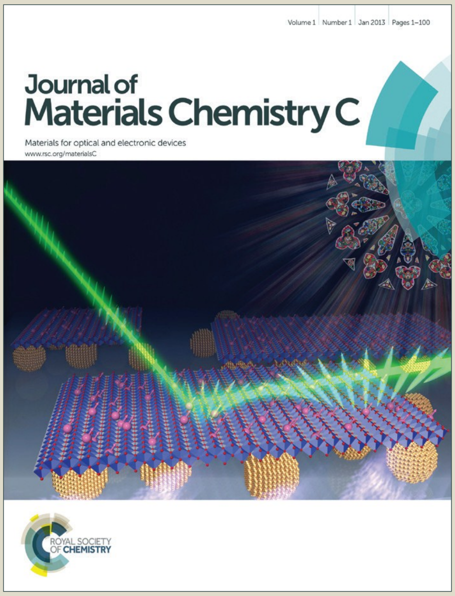

Volume 1 | Number 1 | Jan 2013 | Pages 1–100

Journal of Materials Chemistry C

Materials for optical and electronic devices

www.rsc.org/materialsC

ROYAL SOCIETY OF CHEMISTRY

ROYAL SOCIETY OF CHEMISTRY

www.rsc.org/materialsC

Journal Name

ARTICLE

Sensitizers with Rigidified-Aromatics as the Conjugated Spacer for Dye-Sensitized Solar Cells

Received 00th January 20xx,
Accepted 00th January 20xx

DOI: 10.1039/x0xx00000x

www.rsc.org/

Sumit Chaurasia,[a]† Chia-Jung Liang,[a]† Yung-Sheng Yen,[ab]† Jiann T'suen Lin[a,]*

Metal-free dye sensitized solar cells emerged as an important source of a renewable energy resource because of low production, simple fabrication process and a wide availablility of organic dyes. This review mainly focuses on metal-free sensitizers having rigidifed-aromatics as the conjugated spacer for applications in DSSCs. Based on their structures dyes have been divided into three major subsegments: (i) ladder type polyphenylenes with or without heteroatoms; (ii) rigidfied-aromatics as a donor segments; (iii) fused polyaromatics. Planarization of organic molecules through rigidification of aromatics allows effective communication and their smaller reorganization energy is beneficial to photoinduced charge transfer. Dyes having rigidified aromatics as a conjugated spacer emerged as promising candidates and a maximum efficiency of 12.5 % has been achieved with DSSCs without coadsorbate or co-sensitizer.

1. Introduction

Two decades after Grätzel's seminal report in 2001,[1] significant progress has been made on dye-sensitized solar cells (DSSCs). Though the perovskite-based solar cells which originated from the DSSCs[2] have astonishing boost in conversion efficiency after being transformed to the solid state solar cells or heterojunction solar cells, two major obstacles (toxicity and moisture instability of the active materials) remain to be settled.[3] DSSCs therefore should be still competitive because of simple device fabrication technology and flexibility in molecular design of the sensitizers. Up to now, high power conversion efficiencies of 13.0, 11.50% and 12.5% have been achieved for porphyrin-,[4] polypyridyl Ru(II) complex-[5] and metal-free organic dye-based[6] DSSCs, respectively. Compared with porphyrin and ruthenium dyes, metal-free dyes have two advantages: synthetic feasibility and low cost. Moreover, the efficiency of DSSCs based on metal-free dyes has kept pace with the other two dyes during the past two years, and quite a few dyes have cell conversion efficiency surpassing 10%.[7] The prototype metal-free sensitizer, D-π-A, has an electron donor (D), an electron acceptor (A) which also functions as the anchor for adsorbing on TiO_2, and a conjugated spacer (π) linking the donor and the acceptor. Upon photo-excitation, intramolecular charge transfer (ICT) from the donor to the acceptor will occur with subsequent electron injection into the conduction band of TiO_2. The donor, the acceptor and the conjugated spacer can all be tuned for maximizing the intramolecular charge transfer of the D-π-A molecules.

Compared with the donors and acceptors, there is more variety of the spacer. A good spacer should allow strong electric communication between the donor and the acceptor. This review will be focused on rigidified aromatics (**RGAR**) based on the following reasons: (1) planar spacer can allow more effective electronic communication between the donor and the acceptor; (2) the smaller reorganization energy of a rigid segment is beneficial to photoinduced charge transfer. On the other hand, more planar system may have higher tendency of intermolecular aggregation, which not only reduces the solubility of the sensitizer molecule in common organic solvents, but also quenches the excited state molecule and deteriorates the electron injection. Therefore, rigidified segments are normally accompanied with sterically congested substituents for alleviation of aggregation.

In this review, we define the rigidified aromatics as the fused aromatics or segments comprised of aromatic rings capable of forming quinoidal structure and the number of the aromatic rings in the rigidified segments will be limited to ≧3. Therefore, segments such as naphthylene, fluorene, carbazole, phenothiazine and dithienylcyclopentadiene will be excluded. However, dithieno[3,2-*b*:2′,3′-*d*]thiophene and indenofluorene are included in our discussions. As the rigid aromatic segments have also been successfully used as the electron donor of the sensitizers in several examples, this interesting class of dyes are also discussed briefly at the end of this review.

1.1 Basic operational principle of DSSCs

As shown in Fig. 1, the DSSC device is composed of three adjacent thin layers, including a high band-gap nanocrystalline semiconductor-based mesoporous thin film adsorbed with a dye sensitizer on the working electrode, a platinized counter electrode for the collection of electrons and a redox electrolyte, sandwiched in between the two electrodes. In general it is composed of five materials: 1) a fluorine-doped

---

[a] *Institute of Chemistry, Academia Sinica, Taipei, Taiwan 11529.*
[b] *Assistant Research Scholar of the Ministry of Science and Technology of ROC*
† *The first three authors have contributed equally to this work*

SnO_2 (FTO) glass substrate, 2) a nanocrystalline TiO_2 thin film as a semiconductor, 3) a dye sensitizer, 4) an electrolyte (redox mediator), and 5) a platinum-coated glass substrate. The electrolyte mostly contains I^-/I_3^- redox couple, which is obtained by mixing iodine (I_2) and inorganic or organic iodides in suitable non-aqueous solvents. Fig. 1b describes the operational principle of a typical DSSC. Upon absorption of light [**Equation (1)**], an electron is injected from an excited state of the dye (S*) into the conduction band of the metal oxide [**Equation (2)**]. After percolation through the thin mesoscopic semiconductor film, the electrons are thought to move by a "hopping" mechanism and collected at a transparent conductive substrate of fluorine-doped tin oxide glass (SnO_2:F), on which the TiO_2 film is formed. The electrons then move through the external circuit to the counter electrode (Pt-coated glass). The resultant oxidized dye is subsequently reduced back to its original neutral state by electron donation from the I^- ions in redox mediator. This process is usually called dye regeneration or reduction [**Equation (3)**]. Finally, the I^- ion is regenerated by the reduction of triiodide ion I_3^- at the counter electrode through the donation of electrons from the external circuit [**Equation (4)**] and then the circuit is completed. Ideally, such a cycle is kept repeating without any material being consumed but energy being transformed from light to electricity. During this whole process, there are some undesirable dark reactions or recombination: the electrons injected into the CB of the TiO_2 electrode may recombine either with the oxidized dye [**Equation (5)**], or with I_3^- at the TiO_2 surface [**Equation (6)**], resulting in lowering the photovoltaic performances of DSSCs.

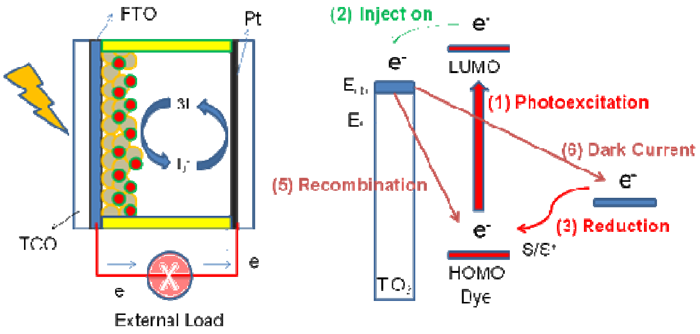

$$S + h\nu \longrightarrow S^* \qquad (1)$$

$$S^* \longrightarrow S^+ + e^- \qquad (2)$$

$$2S^+ + 3I^- \longrightarrow 2S + I_3^- \qquad (3)$$

$$I_3^- + 2e^- \, (Pt) \longrightarrow 3I^- \qquad (4)$$

$$S^+ + e^- \longrightarrow S \qquad (5)$$

$$I_3^- + 2e^- \, (TiO_2) \longrightarrow 3I^- \qquad (6)$$

Fig. 1 (a) Schematic design and (b) working principle of a DSSC.

2. Sensitizers with RGAR in the spacer

2.1. Ladder type Rigidified Aromatics (RGAR) without heteroatoms

In order to reduce the HOMO/LUMO gap of π-conjugated chromophores, thereby shifting the λ_{max} values to longer wavelengths, the following major approaches can be adopted (i) enlargement of the π conjugation, (ii) introduction of aromatic rings with high tendency to form quinoidal structures and (iii) introduction of donor-acceptor substituents to facilitate intramolecular charge transfer transition (Fig. 2). The easiest way to enhance the π-conjugation of phenylene compounds is to extend the conjugation via *para* position. However, large twist angle between the neighbouring phenyl rings will counteract the conjugation of the phenylene compounds. This problem can be solved by locking the neighbouring phenyl rings to a rigid, planar segment. Restricted rotation of the phenyl rings results in better conjugation, for examples, a biphenyl entity vs. a fluorenyl or phenanthrenyl entity.[8] However sometimes these rod like structures shows poor solubility on increasing the number of phenyl units such as Indenofluorene and its higher analogues, which can be easily solved by introducing long hydrocarbon chains onto the sp^3 bridged carbon atoms.[9] For example, ladder type poly(*p*-phenylene)s[10] (**LPPPs**) (Fig. 2) that possess coplanar π-conjugated backbones, obtained through intramolecular annulation have received a considerable amount of research interest. An efficient π conjugation in a fully coplanar **LPPP** backbone leads to a number of interesting properties including increased photoluminescence efficiency[11] and charge mobility.[12] Additionally, enhancing the electron affinity of **LPPPs** was achieved by altering the bridge atoms. **LPPPs** such as indenofluorene (**IF**) and its isomers[13] (Fig. 3), indenoindene,[14] pentaphenylene,[15] and octaphenylene,[16] have been widely used in various fields of organic photovoltaics due to their unique features. In general for D–π–A systems planarization of the conjugated spacer allows more effective electronic communication between the donor and the acceptor.

In this section, we will discuss the use of **LPPPs** as an efficient π–conjugated spacer for DSSCs and their effective length of π–conjugation. Fig. 3 represents the structures of the dyes (**1–21**).

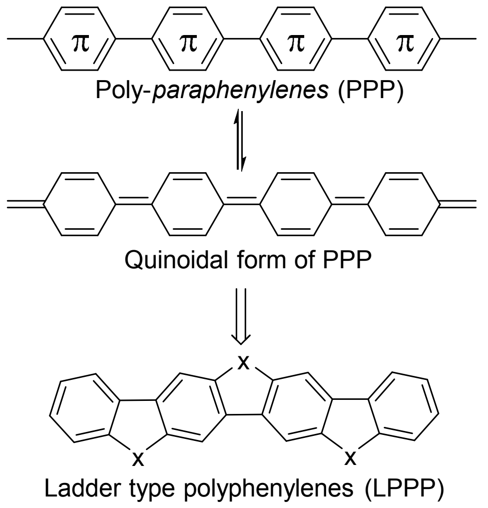

Fig. 2 Approach for enlargement of π-conjugation and ladder type polyphenylenes (LPPP)

Indenofluorene (**IF**), a *para*-terphenyl is considered to be more π–conjugated than fluorene and has been extensively studied in the various fields of organic photovoltaics.[13,17] In 2012, we were the first to report indenofluorene based sensitizers (Fig. 3) for DSSCs with an extended π–groups, a maximum efficiency of 4.05% was obtained with **3**, where indenofluorene was incorporated as a conjugated bridge with an extended π–group furan, diphenylamine as donor, cyanoacrylic acid group as an electron acceptor and anchoring group.[18] Although, the efficiency obtained with indenofluorene based sensitizers (**1**–**3**) was moderate (3.36–4.05%), the findings were interesting as it surpassed the efficiency of pentaphenylene dyes (Fig. 3) reported by Müllen[19] et al. and indaceno[1,2-*b*:5,6-*b*']dithiophene based dyes reported by Yang et al. (Fig. 3).[20] Compared with indenofluorene dyes (**1**–**3**), pentaphenylene dyes[19] **4**–**6** have longer π-conjugation and higher extinction coefficient as evident from their UV absorption spectra (λ_{max} = 442–457 nm, $\varepsilon = 7 \times 10^4$ M^{-1} cm^{-1} for pentaphenylene dyes; λ_{max} = 400–430 nm, $\varepsilon = 5.5 \times 10^4$ M^{-1} cm^{-1} for **IF** dyes), the maximum efficiency of only 2.3% was obtained with the sensitizer **6**. Their inferior performance was attributed to the dominant π–π* character over charge-transfer. Yang et al. reported the indaceno[1,2-*b*:5,6-*b*']dithiophene,[20] a ladder-type π-conjugated heteroacene, where the phenyl ring of indenofluorene is substituted with thiophene with smaller resonance energy in order to achieve high performance photovoltaic materials. Although the indaceno[1,2-*b*:5,6-*b*']dithiophene-based (Fig. 3) dye (**7**) shows better absorption properties than indenofluorene and pentaphenylene dyes, still the maximum efficiency (2.31%) is far inferior than our indenofluorene (**IF**) based sensitizers. Possibly more effective suppression of the dark current, evidenced from the higher photovoltage, results in better cell performance of the indenofluorene dyes.

Polyaromatic compounds or fused aromatics compounds, composed of many fused aromatics rings with big and planar π-conjugations could benefit to the charge transfer and light harvesting when used as a π-bridging unit in a DSSCs.[21] In 2012, our group[22a] was the first to explore the 2,6-linkage mode of anthracene as a rigid planar unit in a DSSC. The choice of 2,6 linkage over 9,10 linkage mode was mainly because of two reasons: (1) the rigid segment has less reorganization energy and may facilitate electron transfer; (2) rigid segments with a planar skeleton may reduce steric congestion and allow more compact dye packing on the TiO_2. However the maximum efficiency of 2.88% was obtained with **10**. Later, we found that the cell efficiency could be greatly improved up to 7.5% if the 2-anthracenyl entity used as the peripheral substituent of the arylamine was replaced with a 2-substituted 9,10-bishexyloxyanthracene entity, **12**–**15** (Fig. 3).[22b] Better suppression of the dye aggregation and dark current are the key to the better performance of these new dyes. An impressively high efficiency (9.11%) surpassing the **N719**-based cell was achieved with the use of CDCA as the co-adsorbent. Under weak light irradiation, the efficiency can be further increased to 10.42%. Very recently, the same concept was explored by Li et al.,[23] who reported four new sensitizers **16**–**19** (Fig. 3) based on the 2,6-linkage mode of anthracene as a rigid planar unit in a DSSCs, with varying substiuents at 9,10 position. Sensitizers **16**–**19** shows efficiency in the range of 5.59–6.42%. The best sensitizer **17** with a stronger donor of hexyloxy-substituted triphenylamine, shows *J*sc 13.42 mA cm^{-2}, *V*oc 722 mV, FF 0.66, and *η* 6.42%, respectively. In comparison, 9,10-conjugated anthracenes normally suffer from larger steric congestion, which jeopardizes the planarity of the conjugated spacer and therefore cell performance.[24] The cell efficiency was raised to 7.03%[24b] only after insertion of an alkynyl entity between the anthracene and the aromatic ring. Jiang et al. reported[25] two new pyrene-based dyes **20** and **21** (Fig. 3). The best dye **20** give a short circuit photocurrent density (*J*sc) of 12.1 mA/cm^2, an open circuit voltage (*V*oc) of 0.71 V, and a fill factor (FF) of 0.71, corresponding to an overall conversion efficiency (*η*) of 6.1% under AM 1.5 conditions with 2 mM of CDCA. These results show the promising design approach of that oligo-conjugated or oligo-aromatic entity is promising as a π-bridging unit of metal free D-π-A sensitizers for DSSCs.

2.2. Ladder type Rigidified Aromatics (RGAR) with heteroatoms

Fig. 4 and Fig. 5 show the structures of the dyes (**22**–**49**) in this category. Hua, Tian and coworkers reported a series of metal-free organic dyes (**22** to **24**) exploiting planar quinacridone (**QA**) and furan moiety as the central π-spacer.[26] Though **QA** is not fused aromatics, the two nitrogen atoms of **QA** allow electronic communication between the donor and the acceptor. Notably, the cells have high photovoltages (776–813 mV) surpassing that of **N719** (726 mV). The DSSCs based on **22** has the best efficiency of 7.70% (*J*sc, 13.2 mA cm^{-2}; *V*oc, 0.804 V; FF, 0.73) with 20 mM of CDCA as the co-adsorbent under AM 1.5 irradiation. The long-term stability of **QA** DSSCs with ionic liquid electrolytes under 1000 h light-soaking was also demonstrated. Kim et al. developed two organic sensitizers (**25** and **26**) containing quinacridone as the electron donor and benzene or thiophene as the π-linker.[27] Dye **25** bearing thiophene as the conjugated bridge showed a larger red-shift with a higher intensity in the intramolecular charge transfer band compared to **26**. The solar cell based on **25** shows a power conversion efficiency of 3.86% (*J*sc, 8.51 mA cm^{-2}; *V*oc, 0.643 V; FF, 0.70). They found that the lower conversion efficiency is due to the two carbonyl groups on quinacridone framework with intense electron-withdrawing property, which compete with cyanoacrylic acid anchoring group and prevent the transfer of localized electrons in the quinacridone moiety, resulting contribution of only shorter absorption wavelength to IPCE.

Indacenodithiophene was found useful as the motif for the sensitizers of polymer solar cells because its coplanarity benefits π-conjugation.[28] Wong and Wu et al. used the indacenodithiophene[29] functionalized with 4-(*n*-hexyloxy)phenyl groups on the sp^3-carbon bridge as the conjugated spacer of the sensitizers, **27**–**29**. The dyes exhibit broad absorption extending to ≧650 nm. The peripheral *n*-hexoxyphenyl side chains on the sp^3–carbon bridge of the core serve as a spatial hindrance to mitigate undesirable dye aggregation. The best efficiency of the cells reaches 6.70% (*J*sc, 13.54 mA cm^{-2}; *V*oc, 0.69 V; FF, 0.71).

In 2014, Cai et al. also employed indacenodithiophene[30] unit as a conjugated spacer and dihexyloxy-subsituted **TPA** as a donor to construct the organic sensitizer **30** for DSSCs. The dyes show very intense and broad absorption. The efficiencies of DSSCs based on volatile solvent electrolyte and solvent-free ionic liquid electrolyte are 7.5% and 6.9%, respectively. The DSSC with the volatile electrolyte was found to have much longer electron lifetime and higher charge collection efficiency. Later, Grimsdale et al. reported cyclopenta[1,2-*b*:5,4-*b*′]dithiophene[31] (**CPDT**)- (**31**–**33**) and cyclopenta[1,2-*b*:5,4-*b*′]dithiophene[2′,1′:4,5]thieno[2,3-*d*]thiophene (**CPDTTT**)-based (**34**–**36**) dyes. The dyes containing **CPDTTT** exhibits more red shifted absorption wavelength and intensity compared to their **CPDT** congeners due to the elongation of π-conjugated bridge. Accordingly, the latter has better cell efficiency than the former with the same donor. An important message in this study is that an electron rich conjugated spacer in combination with a strong donor may lead to unfavourable HOMO level and hamper dye regeneration. Wang et al. reported[32] a sensitizer, **38**, featuring the cyclopenta[1,2-*b*:5,4-*b*′]dithiophene[2′,1′:4,5]thieno[2,3-*d*]thiophene π-linker (**CPDTTT**), which displays an enhanced molar absorption coefficient and a red-shifted absorption peak with respect to its reference dye **37** with the 2,5-di(thiophen-2-yl)thieno[3,2-*b*]thiophene linker. They showed that the charge generation yield of the dye is related to a three dimensional configuration owing to the tethering of four hexylphenyl segments incorporated at the conjugated backbone. The performance of the dyes are dependent upon the dye bath solvent, which has a significant influence on the dye load amounts and some key photovoltaic features such as the photocurrent and photovoltage. The **38**-based cell with the THF and MeCN mixture as dye-bath solvent has the best cell performance: *η*, 8.9%; *J*sc: 15.67 mA cm^{-2}; *V*oc: 0.75 V; FF: 0.756.

Recently, M. -C. Chen et al. reported a series of sensitizers **39**–**42** incorporating a planar tetrathienoacene (**TTA**) unit in the conjugated spacer and 2-cyanoacrylic acid as the electron acceptor.[33] They found that the insertion of the thiophene unit between **TTA** and the 2-cyanoacrylic acid acceptor improves both electron delocalizations as well as self-assembly and dye loading on the TiO_2 surface. In contrast, the insertion of the thiophene between the triphenylamine donor and the **TTA** bridges slightly disrupts molecular backbone planarity, leading to suboptimal dye assembly on TiO_2 and increased recombination losses. The solar cell based on **41** exhibits a power conversion efficiency of 10.1% (*J*sc, 16.5 mA cm^{-2}; *V*oc, 0.833 V; FF, 0.70).

Müllen and coworkers developed two metal-free organic sensitizers **43** and **44** with coplanar dithieno[2,3-*d*;2′,3′-*d*′]benzo[1,2-*b*;4,5-*b*′]dithiophene (**DTBDT**) as the π-spacer.[34] Though coplanarization of the **DTBDT** π-spacer is beneficial for extending the red light response of the sensitizer, lack of any substituent also results in undesirable dye aggregation. **44**-sensitized DSSC with a cobalt electrolyte showed higher conversion efficiency of 6.32%. This was attributed to the better light harvesting and more efficient dark current suppression of **44**.

Wong et al. reported[35] a new class of dyes **45**–**47**, incorporating fused pentaheteroacene or hexaheteroacene functioned as both the donor and the π-bridge with two anchoring groups, the *N*-alkyl bridged helps in improving solubility as well as suppression of dye aggregations. These dyes have impressively high absorption intensity (*ε* >85000 M^{-1} cm^{-1}). The device based on **46** possessing less bulky *N*-alkyl groups has the best efficiency of 5.5% (*J*sc, 13.72 mA cm^{-2}; *V*oc, 0.833 V; FF, 0.58) under AM 1.5 solar irradiation. Xue and coworkers prepared two organic dyes by implementing the dithieno[2,3-*d*:2′,3′-*d*′]thieno[3,2-*b*:3′,2′-*b*′]dipyrrole (**DTDP**) unit into the bridging framework of D-π-A molecules.[36] The **DTDP** dyes, **48** and **49**, have red-shifted ICT bands compared with the dyes containing dithieno[3,2-*b*:2′,3′-d]pyrrole (**DTP**). The better cell performance of **49** than **48** is mainly due to more effective suppression of charge recombination by the hexyloxyphenyl substituents compared with the dihexyl substituents on the **DTDP** unit. Compared to the reference dye **C241**, the sensitizer **49** shows slightly lower cell efficiency under AM 1.5 illumination, 6.6 vs. 7.2%. This mainly originates from the higher regeneration efficiency and charge collection efficiency of the former.

2.3. Rigidifed Polyaromatic Segments: Perylene based Dyes

Perylene, one of the most important polycyclic aromatic hydrocarbons (Fig. 6) was discovered by Kardos in 1913 and has been widely used as the pigment by industries.[37] There are four *peri* and *bay* positions on the perylene core. The *peri*-positions diimide substitution perylenes were developed earlier than the *bay*-poisitions diimide substitution perylenes.

However, most of them exhibited relatively low overall power conversion efficiencies as they were limited to perylene anhydride and perylene imide based dyes.[38]

Ferrere and co-works reported a serious of perylene-based sensitizers, which adsorbed onto TiO_2 via 3,4-dicarboxylic acid anhydride or carboximide group for DSSC. Among them, 9-dioctylaminoperylene-3,4-dicarboxylic acid anhydride (**50**) had the best conversion efficiency (1.92%).[39] Zafer et al. synthesized perylenemonoimide (**51**) dyes with a longer alkyl chain, 6-undecyl group, to afford 1.61% overall conversion efficiency.[40] Odobel et al. studied perylenes with four aryloxy substituents at the bay position and extended the absorbance (λ_{max} = 581 nm) of **52** to longer wavelengths. DSSC based on **76** in an electrolyte consisting of 0.6 M of 1-methyl-3-*n*-propyl imidazolium iodide, 0.1 M of LiI, 0.05 M of I_2 and 0.1 M of 4-*tert*-butyl-pyridine showed cell efficiency of 2.3%.[41] Imahori group synthesized the perylene imide with electron-donating moiety at *bay* positions and a bulky group adjacent to the imide group to suppress the dye aggregation. The efficiency of **53** reached 2.6%.[42] Müllen et al. also published five new perylene molecules with different electron donating group at *peri*- and *bay*- positions. The maximum IPCE of the dye with diarylamine substituted **54** was found over 70% in the range of 480–550 nm, and the efficiency reached 3.9%.[43] To further develop the efficiency of perylene dye, the same group investigated the thiophenyl-perylene **55** and increased the PCE of the cell to 6.8%. The *V*oc, *J*sc and FF of the cell are 728 mV, 12.60 mA cm^{-2}, and 0.74, respectively.[44] Müllen et al. further studied perylene dyes with increasing order of molecular size, **54** < **56** < **57**.[45] The dye of larger size had lower cell efficiency due to lower dye loading under 1 sun irradiation. Under 0.1 sun irradiation, the three dyes had comparable cell efficiency, suggesting the importance of the dye morphology on device performance. Mathew et al. synthesized 1,6,9-tris(triarylaminoalkynyl)perylene monoanhydride (**58**) which containing three electron-donating groups by using Sonogashira cross coupling reaction, and achieved the power conversion efficiency of 2.9% after 6 hours of dye-soaking.[46] Keerthi et al. reported that tetra-TPA-substituted perylene monoanhydride (**58a**) with a broad absorption up to 750 nm (λ_{max} = 624 nm) had a higher cell efficiency than tri-TPA-substituted perylene monoanhydride.[47] Both cells had low efficiencies because the larger molecular size diminished the dye concentration on the TiO_2 surface.

In the past decade, *N*-annulated-perylene (**PNP**) derivatives have been becoming more popular segment for developing metal free sensitizers for DSSC, owing to the tunable optical or electronic property, the easily synthetic pathway and high efficiency. Push–pull type sensitizers by using **PNP** as a new rigid and coplanar π-linker is recently explored by Wu and Wang independently (Fig. 7 and Fig. 8), and both of them have achieved efficiency surpassing the champion dye **YD2**-o-**C8**.

Zhang et al. reported a new metal-free dye (**59**) consisting of *N*-annulated perylene segment as a spacer, diarylamine as a donor and the 2-cyanoacrylic acid as acceptor, to afford 8.8% power conversion efficiency with *J*sc of 14.90 mA/cm^{-2}, a *V*oc of 844 mV by using non-corrosive cobalt redox shuttle.[48a] The same group also reported a new metal-free dye (**60**) consisting of *N*-annulated perylene segment as a spacer, diarylamine as a donor and a benzothiadiazole-benzoic acid as an acceptor. The efficiency of the cell is up to 7.3% with a *V*oc of 788 mV, a *J*sc of 12.63 mA/cm^{-2} and an FF of 0.74.[48b] Replacement of benzothiadiazole in **60** with a more electron-deficient pyridothiadiazole decreased the conversion efficiency to 5.0% due to the diminished electron injection efficiency. Later, Yan et al. in the same group used palladium catalyzed cross-coupling reactions to combine triarylamine and *N*-annulated perylene and synthesized dyes **61** and **62** which possessed narrow HOMO/LUMO gap. Compared with **61**, **62** has a red-shifted maximum absorption wavelength (540 nm) and a lower dye loading amount. DSSC based on **61** had a higher efficiency (9.0%) than **62** (8.6%).[49] Recently, a metal-free perylene dye (**63**) which employed ethynylbenzothiadiazole-benzoic acid instead of cyanoacrylic acid as the electron acceptor achieved high cell efficiency 10.4% (*V*oc = 788 mV; *J*sc = 12.63 mA/cm^{-2}; FF = 0.74).[50] In a very recent article an indeno[2,1-*b*]perylene (**NIP**) dye (**64**) reached the maximum efficiency of 12.5% without the use of any coadsorbate.[6] Though **64** has a longer rigid coplanar system than its previous derivatives, the branched 2-hexyldecyloxy chain incorporated at the insoluble rigid NIP and the flexible alkyl chains introduced to the amine site significantly improve the solubility of the dye and suppress dye aggregation. Wu et al. used **PNP** as the donor of prohpyrin dyes, **65** and **66**.[51] Co(II/III)-based DSSCs of **65** and **66** display power conversion efficiencies as high as 10.3% and 10.5%, respectively, which is comparable to that of the **YD2**-o-**C8** cell (10.5%) under the same conditions. In continuation, Wu et al. published three novel push pull type dyes **67**–**69** and a maximum efficiency of only 6.95 % was obtained.[52] Wang et al. reported four new perylene dyes[53] **70**–**73** where the *N*-annulated perylene was used as the rigidified spacer and the DSSCs exhibited overall conversion efficiencies ranging from 4.90% to 8.28% under AM 1.5 solar conditions. The best efficiency was obtained with **73** when the anchoring group was directly attached to the perylene moiety.

2.4. Rigidified Aromatics Segments: Quinoxaline and Benzothiadiazole/Benzoxazole based dyes

Fig. 9 and Fig. 10 represent the structures of the dyes (**74**–**104**) in this category. In order to expand the absorption band of the dye, Zhou et al. constructed an organic dyes **76** with a coplanar dithieno[2,3-*a*:3′,2′-*c*]phenazine entity by replacing the benzene rings of the phenazine core with the thiophene rings.[54] Compared to the reference dyes, **74** and **75**, the absorption spectrum of **76** covers the whole visible region and extends to the NIR region. After optimizing the molar ratio between **76** and **74,** the co-sensitized quasi-solid-state DSSCs showed a higher *η* of 8.04%, as compared to that sensitized by either **76** (5.28%) or **74** (7.03%). The results are attributed to the complementary absorption spectra of the two sensitizers.

Zhou and co-workers also reported **77** and **78** with a acenaphtho[1,2-*b*]thieno[3,4-*e*]pyrazine unit in the conjugated backbone.[55] Compared with the thieno[3,4-*b*]pyrazine-based congener, these acenaphtho[1,2-*b*]thieno[3,4-*e*]pyrazine dyes exhibit bathochromic shift of the absorption spectra. It is impressive that the IPCE spectra of these two dyes cover the whole visible range extending into the NIR region up to 900 nm. Such a broad absorption is greatly beneficial to the improvement of photocurrent density and power-conversion efficiency. However, **77** and **78** exhibit low *V*oc values (below 500 mV), which partially counteract the positive effect of the near infrared (NIR) IPCE response, resulting in moderate PCEs of 5.3 and 3.66%, respectively. Nevertheless, the cell of **77** maintained an almost constant power conversion efficiency under one-sun soaking for 1000 h.

Wong et al. reported four organic dyes using naphtho[2,1-*b*:3,4-*b*′]dithiophene entity as the π-spacer.[56] They demonstrated that the molecule with two naphtho[2,1-*b*:3,4-*b*′]dithiophene entities as the π-linker has broader absorption, and the highest *J*sc among the four dyes. The devices based on the four molecules have moderate efficiencies of 4.38 ± 0.12% (**79**), 3.98 ± 0.12% (**80**), 4.60 ± 0.16% (**79a**), and 4.49 ± 0.16% (**80a**), respectively.

Cao and coworkers reported four D–π–A metal-free organic dyes, **81**–**84**, which contained a dithienopyrrolobenzothiadiazole (**DTPBT**) unit in the conjugated spacer linking the arylamine donor and the 2-cyanoacrylic acid acceptor.[57] **DTPBT** is a planar fused segment consisting of both electron rich entity and electron deficient entity (benzothiazole). These dyes have broad absorption in the visible region and a very intense ICT band (ε > 42000 M^{-1} cm^{-1}). Due to strong intermolecular interactions, π–π stacking of the dyes, CDCA was needed as the co-adsorbent during dye soaking of TiO_2 for better cell performance. The dye (**84**) with triphenylamine as the donor exhibits better photovoltaic performance than **81**–**83** having phenothiazine as the donor. The conversion efficiencies are 6.86% and 7.55% for the cells without and with CDCA (1 mM), respectively, under standard AM 1.5 solar irradiation.

Shi et al. introduced a rigid conjugated unit, 11,12-bis(hexyloxy)dibenzo[*a*,*c*]phenazine[58] (**BPz**), between the triphenylamine donor and the 2-cyanoacrylic acid acceptor/anchor to construct organic sensitizers **85**–**87**. These dyes belong to the so called ‘‘D–A′–π–A’’ sensitizers[59] with **BPz** as the auxiliary acceptor. The two hexyloxy substituents are on the orthogonal directions with planar configuration, which avoids dye aggregation. Therefore, high performance DSSCs can be achieved without co-adsorbent. Dye **87** shows the best η of 7.20%.

Lin et al. synthesized a series of new dyes containing dithieno[3′,2′:3,4;2′′,3′′:5,6]benzo[1,2-*c*]furan (**DTBF**) entity in the conjugated spacer, **88**–**91**.[60] These dyes showed *J*-aggregation in the thin film, which is beneficial to the light-harvesting. Under AM 1.5 irradiation, the cell of **91** adding 10 mM CDCA as the coadsorbent showed the best performance with a *J*sc of 14.29 mA cm^{-2}, a *V*oc of 0.76 V and a fill factor (FF) of 0.66, corresponding to an overall conversion efficiency of 7.33%.

To further improve the light-harvesting and alleviate the dye aggregation and charge recombination, Lin et al. reported new sensitizers, **92**–**96** featuring dithieno[3,2-*f*:2′,3′-*h*]quinoxaline (**DTQ**) as the π-linker.[61] The planarized and electron-deficient **DTQ** unit is advantageous for red-shifting of the absorption spectrum. DSSCs based on these dyes showed efficiencies in the range 6.11% to 7.59%. Moreover, when the dye **92** was co-adsorbed with threefold of CDCA, the cell efficiency reached 8.41%, which is higher than that of the **N719**-based standard cell (8.27%) under AM 1.5 irradiation.

Reynolds and coworkers developed quadrupolar D_2A dyes **97**–**99** containing dithienophenazine as the π-spacer and thiophene as the electron donor for DSSC application[62] Two isomers, dithieno[2,3-*a*:3′,2′-*c*]phenazine and dithieno[3,2-*a*:2′,3′-*c*]phenazine, employed as core unit to construct the organic dyes for DSSCS. They demonstrated that the isomerism of the dyes affected the optical property and cell performance. The results show that increasing the number of internal thiophene from two to six units enhances the open circuit voltage and the short circuit current.

Reynolds and coworkers further explored the structure-property relationships of the dithienophenazine (**DTP**) and dibenzophenazine (**DBP**) acceptor units for DSSCs.[63] Two external thiophene units were covalently attached to the core at two different positions for **DBP**, together with two isomers for **DTP** lead to a set of four isomeric structures (**100**–**102)**, as shown in Fig. 10. The **DTP** dyes have a smaller energy gap, a higher HOMO energy level and greater fluorescence and nonradiative rate constants in solution when compared to the DBP congeners. When integrated into DSSCs, the *V*oc is ~80 mV greater for the **DBP**s, and this change is likely due to an increase of the TiO_2 conduction band. DSSCs based on these dyes showed efficiencies in the range 0.53% to 0.73% without the use of additives or scattering TiO_2 layers.

Yang et al. reported[64] two novel donor–acceptor organic dyes (**103** and **104**) with pyrazino-[2,3-*f*][1,10]phenanthroline (**PPL**) as an electron-withdrawing anchoring group. **103** and **104** can be efficiently adsorbed on the TiO_2 surface through the anchoring group, and the **104**–based cells showed a highest power conversion efficiency of 4.04%, indicating that **PPL** is a promising building block with dual functions, acceptor and anchor, for carboxylic acid free organic dyes.

3. Rigidified Aromatic segments as a donor

In addition to the rigidified aromatic segments discussed in the previous sections, several rigidified aromatic segments have electron-rich nature which make them as good electron donors and have been tested for their applicability in DSSCs. Fig. 11 and Fig. 12 show the structures of the dyes (**105**–**128**) in this category. Islam, Jin and coworkers incorporated thieno[2,3-*a*]carbazole as a donor and thiophene or furan as a π-linker to produce **105** to **109**.[65] The organic sensitizers **107** and **108** having long *n*-octyl chain and bulky substituents on the donor unit have red-shifted intramolecular charge transfer absorption bands and higher maximal IPCE values compared with that of **109**. Among the dyes, the DSSCs based on **109** yielded an overall conversion efficiency up to 7.4%, which was attributed to the efficient suppression of the charge recombination and intermolecular π−π interaction due to introduction of hexyl chains on the thienyl units.

Carbazole was used by Koumura and co-workers as the electron donor of the sensitizers with good performance.[66] Later, the same group used a segment with two fused carbazole units, 5,11-dioctylindolo[3,2-*b*]carbazole moiety, as the electron donor.[67] Similar to the carbazole, the indolo[3,2-*b*]carbazole also has rigid planar geometry, however, the latter is a better donor due to the presence of extra nitrogen atom. The nitrogen atoms allow incorporation of hydrophobic long alkyl chains, which not only improve the solubility of the dyes, but also prevent water-induced dye desorption from the TiO_2 surface. Hara et al. designed two new sensitizers **110** and **111**,[67] in which indolo[2,3-*b*]carbazole was used as a donor and *n*-hexyl-subsituted oligothiophene as a π-spacer. DSSCs based on the sensitizer **110** outperform that of **111** even though the former has smaller π-conjugation. DSSC based on sensitizer **110** gave a short-circuit photocurrent density (*J*sc) of 15.4 mA cm^{-2}, an open-circuit voltage (V_{oc}) of 0.71 V, and a fill factor (FF) of 0.67, corresponding to an overall conversion efficiency (η) of 7.3%. Both dyes showed remarkable cell stability, and the cells retained the initial efficiency even after 600 h of continuous visible-light irradiation at 50 °C. The remarkable stability of dyes, **110** and **111**, was attributed to the hydrophobic long *n*-octyl and *n*-hexyl aliphatic chains, which could prevent water-induced dye desorption from the TiO_2 surface. Compared to triphenyl amine, indolo[3,2,1-*jk*]carbazole (**IC**) structure has a better planarity and rigidity. However the dyes based on **IC**, **112** and **113** showed inferior power conversion efficiency of 3.96 and 2.85%.[68] A similar series of new rigidified donors based on azacyclazine scaffold was synthesized by Ganguly and his coworkers.[69] However, cell performance was not reported.

Tian et al. also witnessed the donating ability of the indolo[2,3-*b*]carbazole entity. The sensitizers prepared, **114**–**117**, were composed of indolo[2,3-*b*]carbazole as the donor, cyanoacrylic acid as the acceptor and benzothiadoazole, thiophene or thienothiophene as the π-spacer.[70] These dyes have very intense π–π* and intramolecular charge transfer absorption bands. Introduction of benzothiazdiazole unit was found to red shift the absorption spectra. It is also interesting that introduction of benzothiazdiazole or thieno[3,2-*b*]thiophene increases the photo-stability of the dyes. The **117** showed a cell efficiency of 7.03% (J_{SC} of 14.81 mA cm^{-2}, V_{OC} of 0.69 V and FF of 0.69). Photo-stable indolo[2,3-*b*]carbazole dyes, **118**–**120**, were also developed via similar approach by Su's group.[71] Among these dyes, **118** showed the best conversion efficiencies of 6.53% and 7.49% using 4 μm and 8 μm scattering layers, respectively.

Later, Su reported indolo[2,3-*b*]carbazole dyes with a diketopyrrolopyrroles (**DPP**) entity in the conjugated spacer,[72] the hydrocarbon chains at both indolo[2,3-*b*]carbazole and **DPP** were proved to be an effective strategy for reducing the π−π aggregation of the dyes on TiO_2 and suppressing the charge recombination. The cell efficiencies are 8.24 and 7.83% for **121** (J_{SC}, 15.72 mA cm^{-2}; V_{OC}, 0.739 V; FF, 0.71) and **121a** (J_{SC}, 14.85 mA cm^{-2}; V_{OC}, 0.765 V; FF, 0.69), respectively. The better performance of **121** was attributed to the better light harvesting of the former.

Thomas and coworkers reported dyes **122a**–**122e** possessing indolo[2,3-*b*]quinoxaline as the donor in the organic sensitizers construction.[73] They found that the optical and photovoltaic properties are mainly dependent on the nature of the π-linker. The solar cell performances based on these dyes are in the range from 0.86% to 3.45% depending on the π-linker.

Recently, Wong et al. reported a dianchor organic dye (ICZDTA) containing 5,7-dialkylindolo[2,3-*b*]carbazole entity, via a double intramolecular Buchwald−Hartwig reactions.[74] Being the isomer of indolo[2,3-*b*]carbazole, 5,7-dialkylindolo[2,3-*b*]carbazole is also a rigid coplanar donor. Theoretical calculation indicates efficient electron transfer from **123** to TiO_2 upon photo-excitation. The solar cell based on the **123** sensitizer delivers a conversion efficiency of 6.02%.

Zheng et al. designed and synthesized a series of metal-free organic dyes, **124**–**126**, containing the carbazole-like segment benzo[*a*]carbazole as the electron donor and furan or thiophene as the π-linker.[75] The dye **126** showed a broad IPCE response with a photocurrent signal up to ~740 nm. Accordingly, **126** gave the best photovoltaic performance with (*J*sc, 14.8 mA cm^{-2}; *V*oc, 0.744 V; FF of 0.68), and an overall power conversion efficiency of 7.54% under AM 1.5 G irradiation.

Coplanar benzo[*b*]naphtho[2,1-*d*]thiophene synthesized via iodine-mediated cascade cyclization of the thioanisole-substituted aryldiynes[76] was used as the donor of the sensitizer, **127**, by Yamamoto and coworkers. The cell showed a moderate conversion efficiency of 3.3% (*J*sc, 7.04 mA cm^{-2}; *V*oc, 0.653 V; FF, 0.728).

Incorporating a planar amine with bulky substituents[77] was found to not only increase the life of the charge-separated state of the dyes by the delocalization of the generated cation over a planar amine unit but also inhibit dye aggregation. Ko et al. reported a novel class of organic sensitizers,[78] where the triphenylamine donor was rigidified using carbon bridges with alkyl or alkoxy chains, and connected to an electron-acceptor by thiophene units. Dye **128** with hexyl chains onto the planarized amine has the best cell performance: *J*sc, 16.78 mA cm^{-2}; *V*oc, 0.75V; FF, 0.70; η, 8.71%. The efficiency is much higher than their reference dye containing triphenylamine as a donor (η = 6.0%).

Conclusions

This paper summaries the importance of rigidified aromatic systems as a conjugated spacer, either in a ladder form or fused polyaromatic. In the ladder form the π–π* transition character of the dye generally becomes more dominant over charge transfer beyond a certain number of benzene ring fused together via sp^3 bridged carbon atoms. This makes the higher analogues to have inferior performances. However, introduction of heteroatoms in place of sp^3 bridged carbon atoms showed impressive efficiencies. Rigidified polyaromatic systems with or without heteroatoms tend to have broad and intense absorption, which is beneficial to the light harvesting. Several *N*-annulated perylene and analogues-based sensitizers, when used as the electron donor or conjugated spacer, have been reported to have high DSSC performance. Without use of any coadsorbate, a sensitizer consisting of an *N*-annulated indenoperylene donor and a secondary acceptor achieved the record efficiency of 12.5%, which surpassed the champion dye **YD2**-o-**C8**. The conjugated segment with planar fused segments consisting of both electron rich entity and electron deficient entity are also promising as the spacer because of the broadened absorption spectra. Better cell performance based on sensitizers with rigidified aromatics can be anticipated.

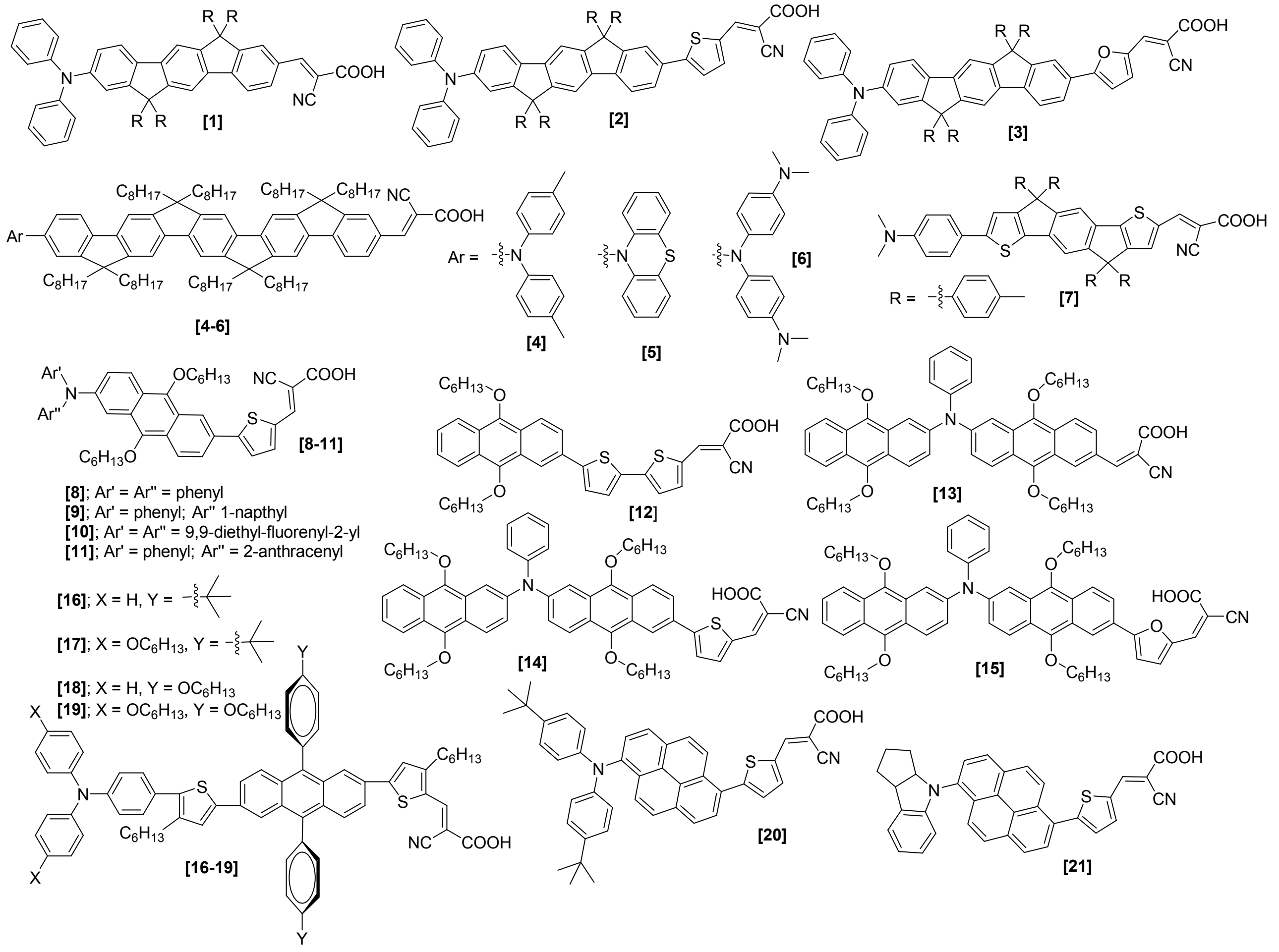

Fig. 3 Dyes **1**-**21** based on LPPPs rigidified aromatics without heteroatoms.

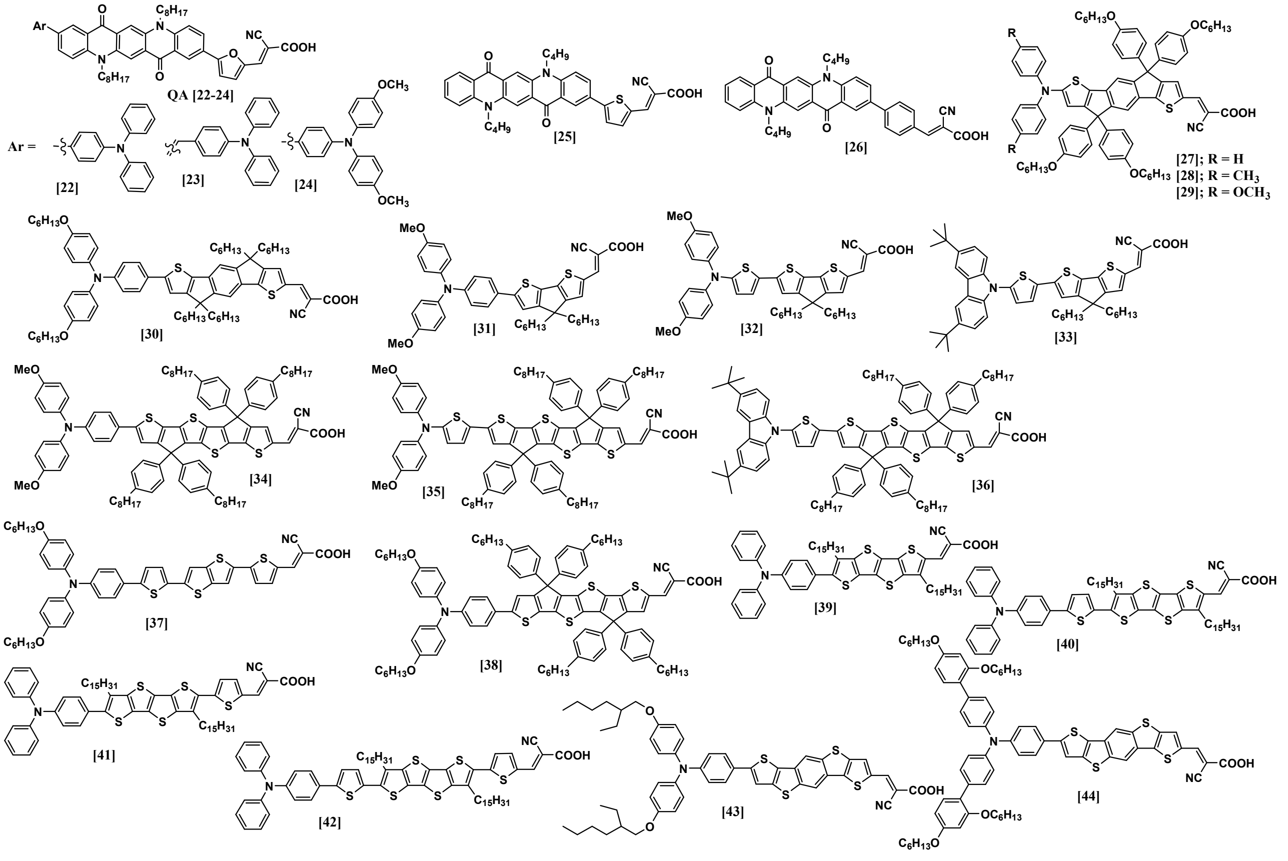

Fig. 4 Dyes **22**-**44** based on LPPPs rigidified aromatics with heteroatoms.

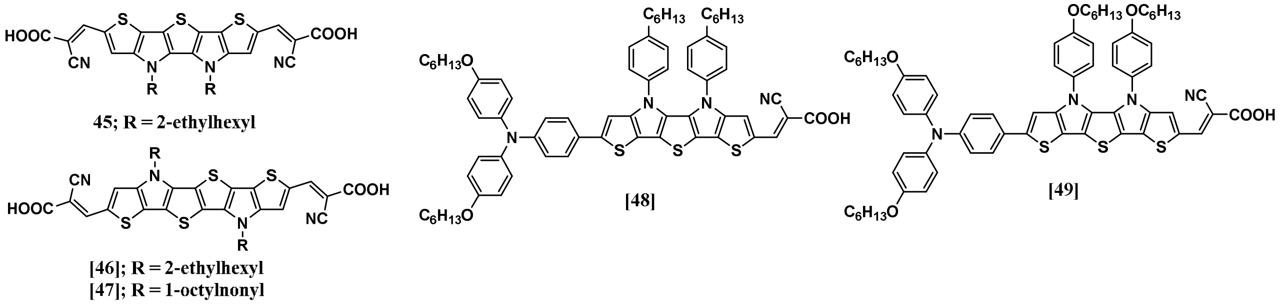

Fig. 5 Dyes **45**-**49** based on rigidified aromatics with heteroatoms.

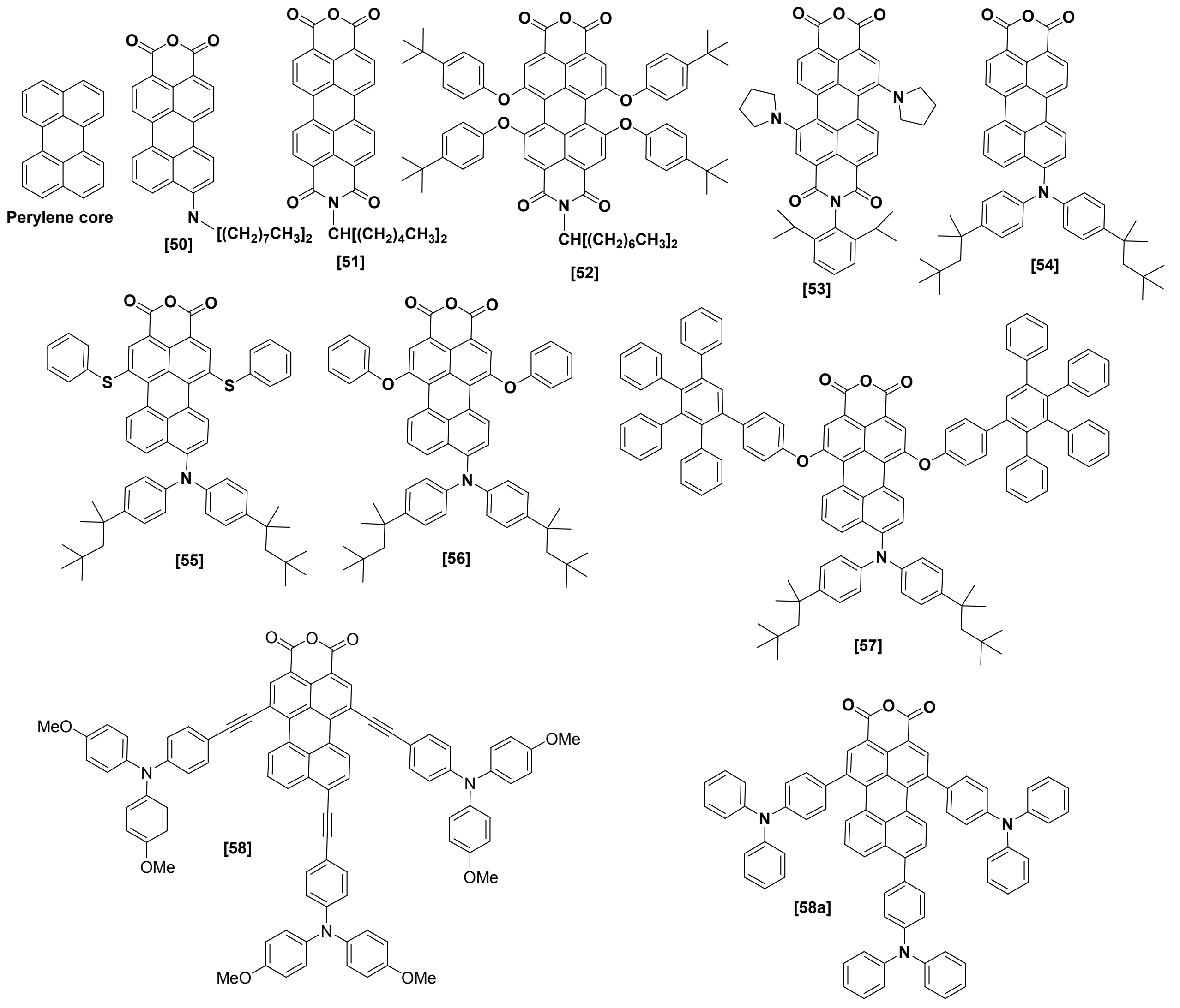

Fig. 6 Perylene dyes **50**-**58a**.

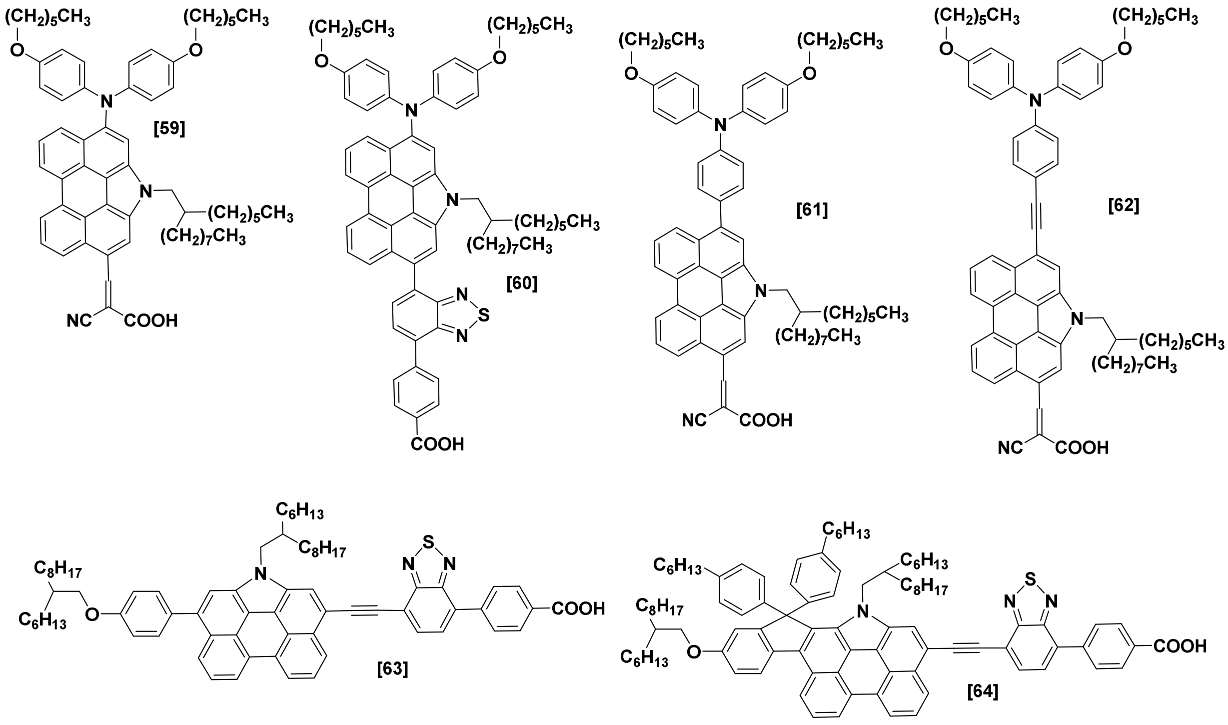

Fig. 7 *N*-Annulated-perylene dyes **59**-**64**.

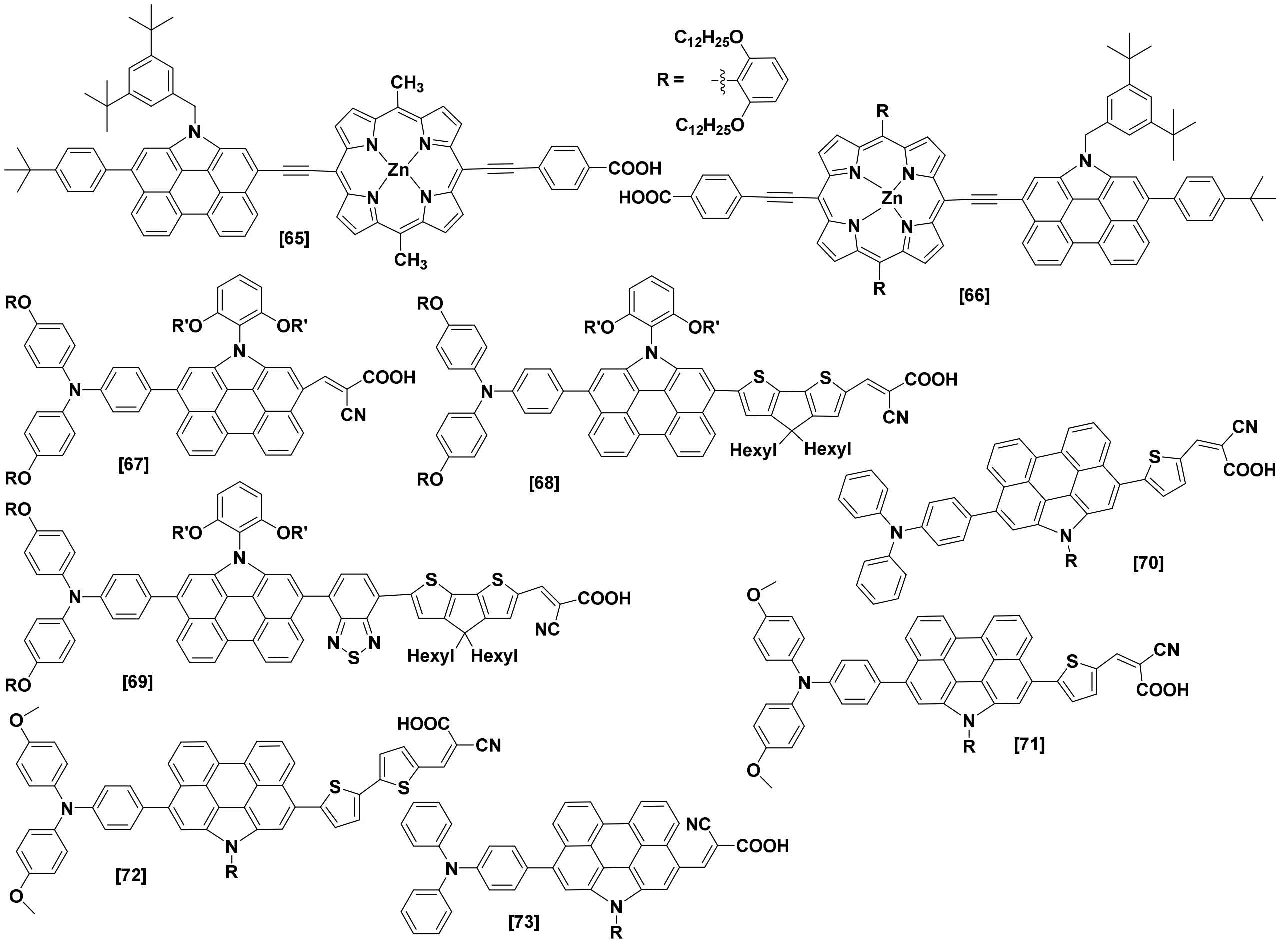

Fig. 8 *N*-Annulated-perylene perylene dyes **65**-**73**.

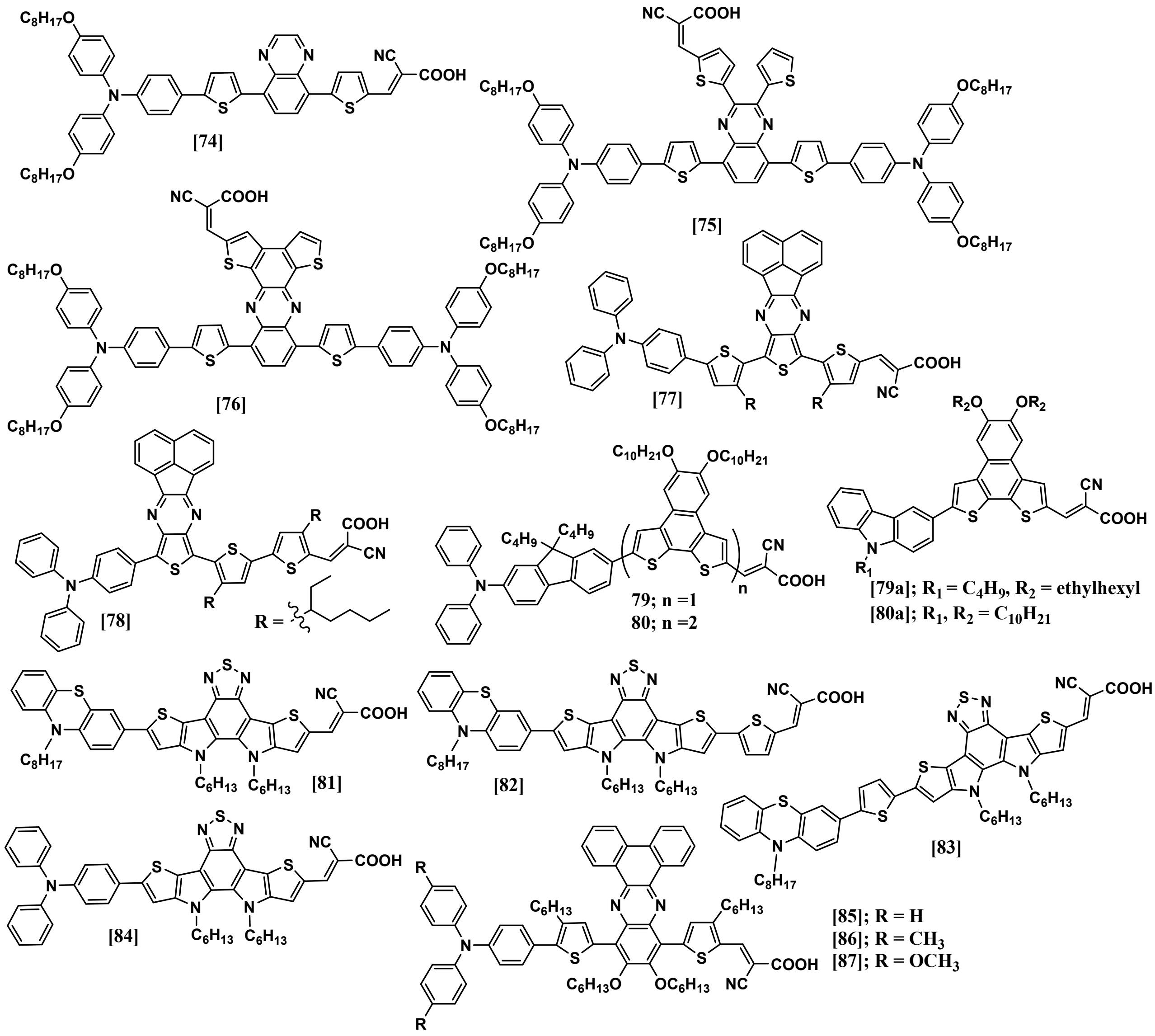

Fig. 9 Rigidified polyaromatics: quinoxaline and benzothiadiazole based dyes **74**-**87**.

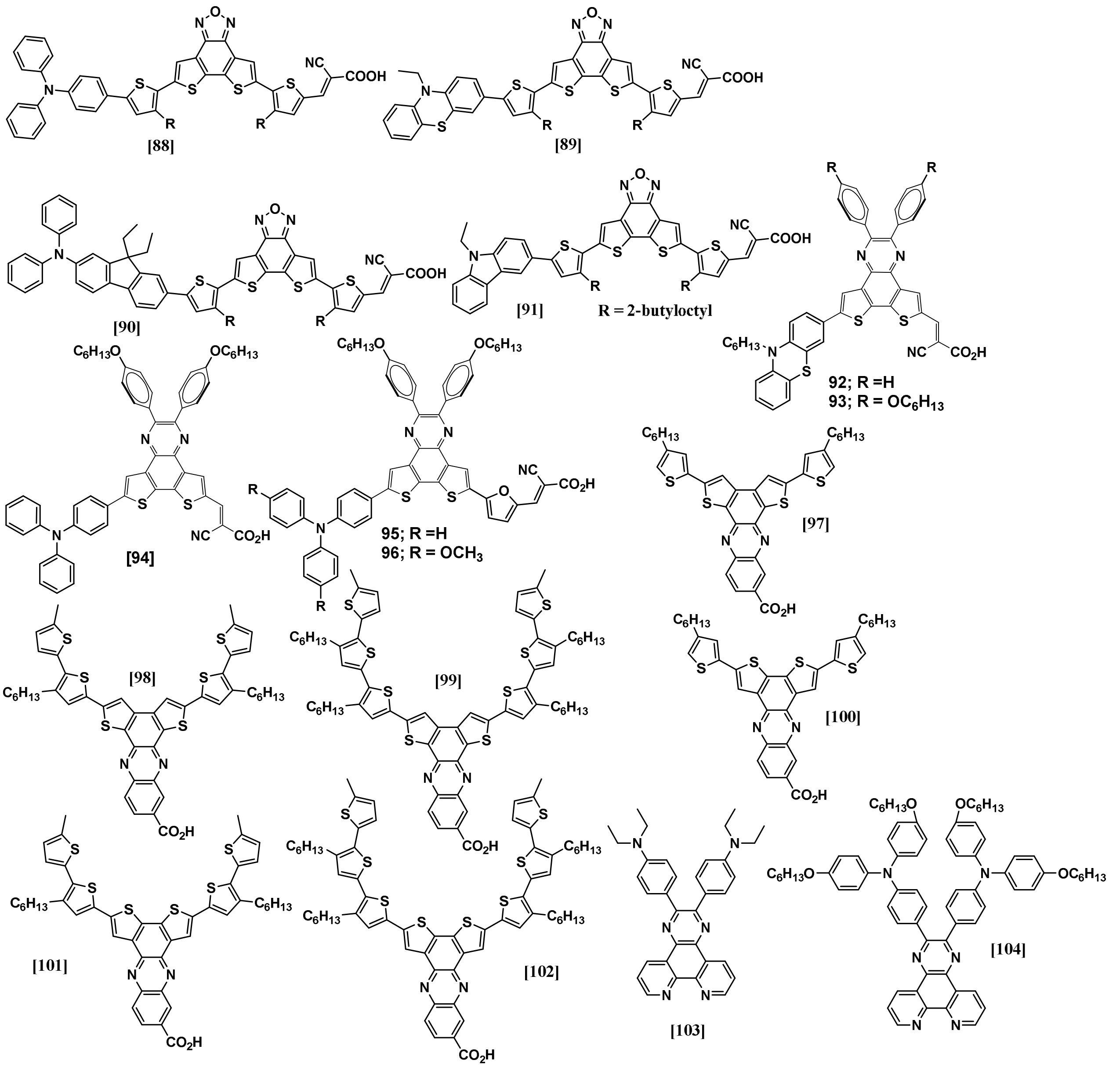

Fig. 10 Rigidified polyaromatics: quinoxaline and benzooxazole based dyes **88**-**104**.

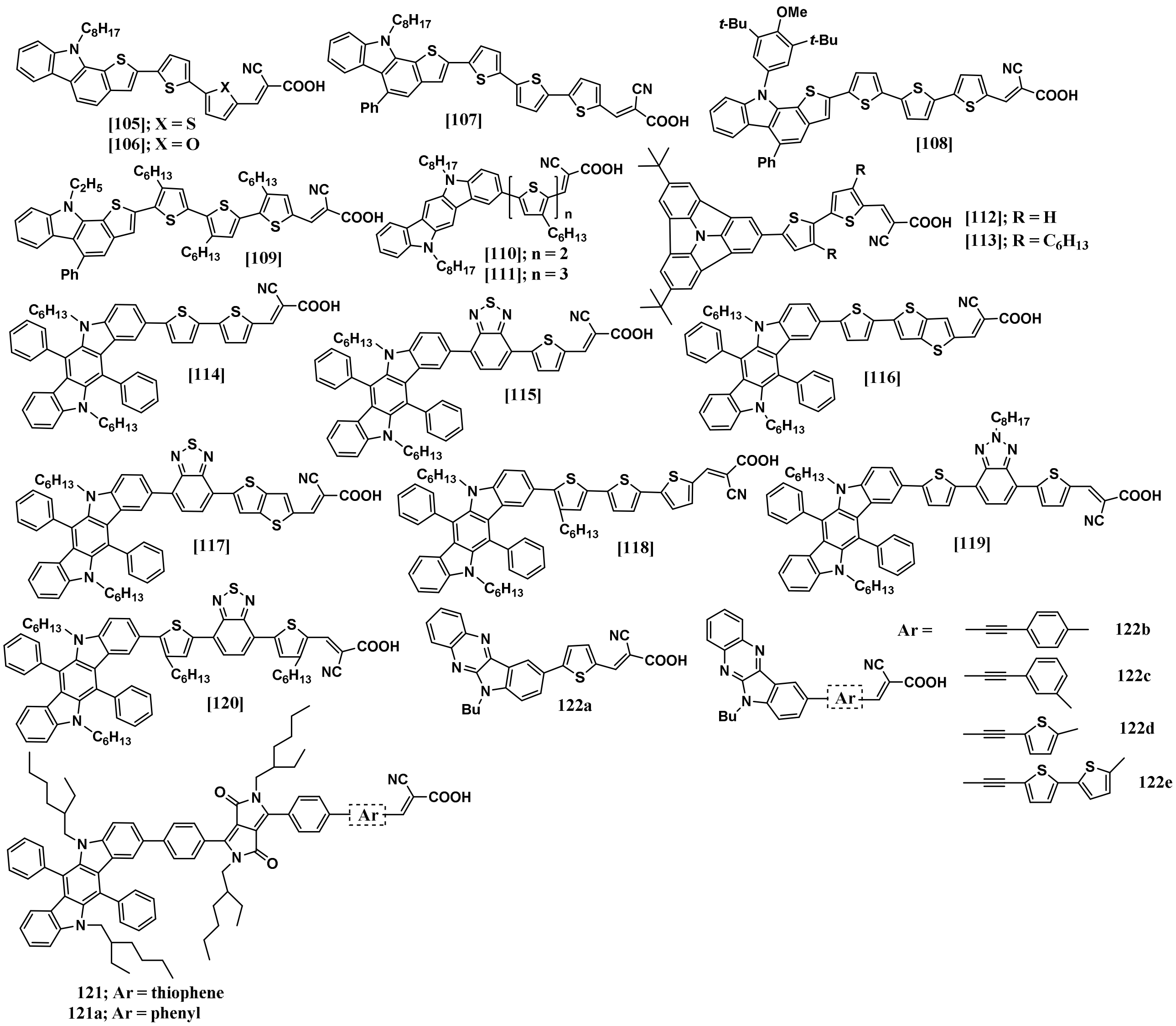

Fig. 11 Sensitizers **105**-**122e** with a rigidified aromatic segment as the donor.

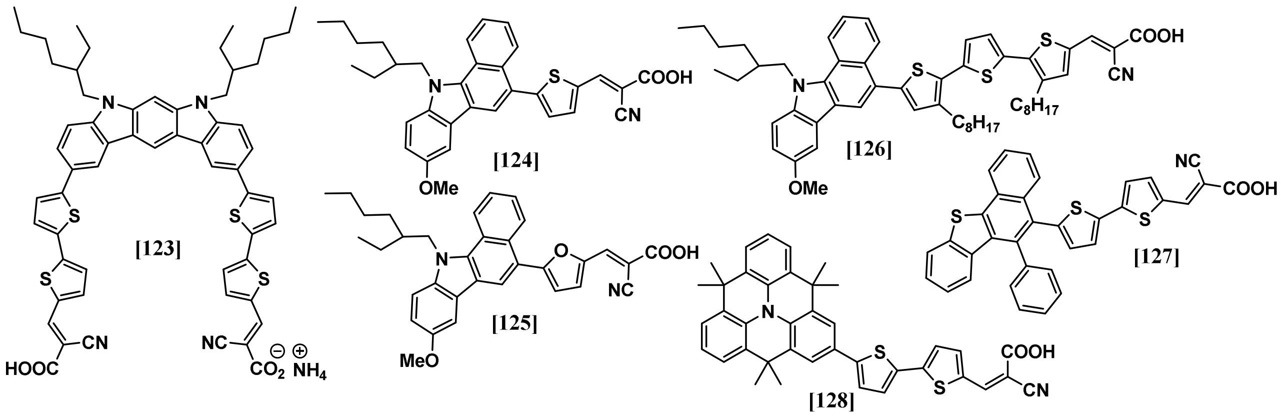

Fig. 12 Sensitizers **123**-**128** with a rigidified aromatic segment as the donor.

Acknowledgements

We would like to acknowledge the Institute of Chemistry, Academia Sinica, and the Ministry of Science and Technology, Taiwan, for their financial support.

References

1 B. O'Reagen and M. Grätzel, *Nature*, 1991, **353**, 737–740.

2 A. Kojima, K. Teshima, Y. Shirai and T. Miyasaka, *J. Am. Chem. Soc.*, 2009, **131**, 6050–6051.

3 (a) P. Gao, M. Grätzel and M. K. Nazeeruddin, *Energy Environ. Sci.*, 2014, **7**, 2448–2463; (b) S. Kazim, M. K. Nazeeruddin, M. Grätzel and S. Ahmad, *Angew. Chem., Int. Ed.*, 2014, **53**, 2812–2824; (c) S. D. Stranks, P. K. Nayak, W. Zhang, T. Stregiopoulos and H. J. Snaith, *Angew. Chem., Int. Ed.*, 2015, **54**, 3240–3248; (d) T.-B. Song, Q. Chen, H. Zhou, C. Jiang, H.-H. Wang, Y. Yang, Y. Liu, J. You and Y. Yang, *J. Mater. Chem. A*, 2015, **3**, 9032–9050.

4 S. Mathew, A. Yella, P. Gao, R. Humphry-Baker, B. F. Curchod, N. Ashari-Astani, I. Tavernelli, U. Rothlisberger, M. K. Nazeeruddin and M. Grätzel, *Nat. Chem.*, 2014, **6**, 242–247.

5 C.-Y. Chen, M. Wang, J.-Y. Li, N. Pootrakulchote, L. Alibabaei, C.-H. Ngoc-le, J.-D. Decoppet, J.-H. Tsai, C. Grätzel, C.-G. Wu, S. M. Zakeeruddin and M. Grätzel, *ACS Nano*, 2009, **3**, 3103–3109.

6 Z. Yao, M. Zhang, H. Wu, L. Yang, R. Li and P. Wang, *J. Am. Chem. Soc.*, 2015, **137**, 3799–3802.

7 (a) W. Zeng , Y. Cao, Y. Bai, Y. Wang, Y. Shi, M. Zhang, F. Wang, C. Pan and P. Wang, *Chem. Mater.*, 2010, **22**, 1915–1925; (b) Y. Bai, J. Zhang, D. Zhou, Y. Wang, M. Zhang and P. Wang*, J. Am. Chem. Soc.*, 2011, **133**, 11442-11445; (c) M. Xu, D. Zhou, N. Cai, J. Liu, R. Li and P. Wang, *Energy Environ. Sci.*, 2011, **4**, 4735–4742.

8 I. B. Berlman ed. Handbook of Fluorescence Spectra of Aromatic Molecules, 2nd Ed., Academia Press, New York, 1971.

9 (a) A. C. Grimsdale and K. Müllen, *Adv. Polym. Sci.*, 2006, **199**, 1; (b) A. C. Grimsdale and K. Müllen, *Adv. Polym. Sci.*, 2008, **212**, 1; (c) C. Li, M. Liu, N. G. Pschirer, M. Baumgarten and K. Müllen, *Chem. Rev.*, 2010, **110***,* 6817–6855.

10 (a) U. Scherf, *J. Mater. Chem.*, 1999, **9**, 1853–1864; (b) A. C. Grimsdale and K. Müllen, *Angew. Chem., Int. Ed.*, 2005, **44**, 5592–5629.

11 (a) S. Setayesh, D. Marsitzky and K. Müllen, *Macromolecules*, 2000, **33**, 2016–2020; (b) J. Jacob, J. Zhang, A. C. Grimsdale, K. Müllen, M. Gaal and E. J. W. List, *Macromolecules*, 2003, **36**, 8240–8245.

12 D. Hertel, U. Scherf and H. Bässler, *Adv. Mater.*, 1998, **10**, 1119–1122.

13 (a) A. G. Fix, P. E. Deal, C. L. Vonnegut, B. D. Rose, L. N. Zakharov and M. M. Haley, *Org. Lett.*, 2013, **15**, 1362–1365; (b) T. Hadizad, J. Zhang, Z. Y. Wang, T. C. Gorjanc and C. Py, *Org. Lett.*, 2005, **7**, 795–797; (c) S. Merlet, M. Birau and Z. Y. Wang *Org. Lett.,* 2002, **4**, 2157–2159; (d) D. Thirion, J. Rault-Berthelot, L. Vignau and C. Poriel, *Org. Lett.*, 2011, **13**, 4418–4421.

14 S. Song, Y. Jin, S. H. Kim, J. Moon, K. Kim, J. Y. Kim, S. H. Park, K. Lee and H. Suh, *Macromolecules*, 2008, **41**, 7296–7305.

15 (a) J. Jacob, S. Sax, T. Piok, E. J. W. List, A. C. Grimsdale and K. Müllen, *J. Am. Chem. Soc.*, 2004, **126**, 6987–6995; (b) J. Jacob, S. Sax, M. Gaal, E. J. W. List, A. C. Grimsdale and K. Müllen, *Macromolecules*, 2005, **38**, 9933–9938; (c) K.-T. Wong, L.-C. Chi, S.-C. Huang, Y.-L. Liao, Y.-H. Liu and Y. Wang, *Org. Lett.*, 2006, **8**, 5029–5032.

16 Y. Wu, J. Zhang and Z. Bo, *Org. Lett.*, 2007, **9**, 4435–4438.

17 M. R. Rao, A. Desmecht and D. F. Perepichka, *Chem. Eur. J.*, 2015, **21**, 6193–6201.

18 S. Chaurasia, Y.-C. Chen, H.-H. Chou, Y.-S. Wen and J. T. Lin, *Tetrahedron*, 2012, **68**, 7755–7762.

19 G. Zhou, N. Pschirer, J. C. Schöneboom, F. Eickemeyer, M. Baumgarten and K. Müllen, *Chem. Mater.*, 2008, **20**, 1808–1815.

20 J. Kim, Y. Jo, W.-Y. Choi, Y. Jun and C. Yang, *Tetrahedron Lett.*, 2011, **52**, 2764–2766.

21 (a) G. Zhang, H. Bala, Y. Cheng, D. Shi, X. Lv, Q. Yu and P. Wang, *Chem. Commun.*, 2009, **45**, 2198–2200; (b) M. Xu, D. Zhou, N. Cai, J. Liu, R. Li and P. Wang, *Energy Environ. Sci.*, 2011, **4**, 4735–4742; (c) Y. Cao, N. Cai, Y. Wang, R. Li, Y. Yuan and P. Wang, *Phys. Chem. Chem. Phys.*, 2012, **14**, 8282–8286; (d) S. Jiang, X. Lu, G. Zhou, Z.-S. Wang, *Chem. Commun.*, 2013, **49**, 3899–3901.

22 (a) Y.-S. Yen, Y.-C. Chen, H.-H. Chou, S.-T. Huang and J .T. Lin, *Polymers,* 2012, **4**, 1443–1461; (b) R. Y.-Y. Lin, H.-W. Lin, Y.-S. Yeng, C.-H. Chang, H.-H. Chou, P.-W. Chen, C.-Y. Hsu, Y.-C. Chen, J. T. Lin and K.-C. Ho, *Energy Environ. Sci.*, 2013, **6**, 2477–2486.

23 H. Li, Y. Yang, Y. Hou, R. Tang, T. Duan, J. Chen, H. Wang, H. Han, T. Peng, X. Chen, Q. Li and Z. Li, *ACS Sustainable Chem. Eng.*, 2014, **2**, 1776–1784.

24 (a) K. Srinivas, K. Yesudas, K. Bhanuprakash, V. J. Rao and L. Giribabu, *J. Phys. Chem. C*, 2009, **113**, 20117–20126; (b) C. Teng, X. C. Yang, C. Yang, S. F. Li, M. Cheng, A. Hagfeldt and L. Sun, *J. Phys. Chem. C*, 2010, **114**, 9101–9110; (c) K. R. J. Thomas, P. Singh, A. Baheti, Y.-C. Hsu, K.-C. Ho and J. T. Lin, *Dyes Pigm.*, 2011, **91**, 33–43.

25 C.-C. Yu, K.-J. Jiang, J.-H. Huang, F. Zhang, X. Bao, F.-W. Wang, L.-M. Yang and Y. Song, *Org. Electron.*, 2013, **14**, 445–450.

26 J. Yang, F. Guo, J. Hua, X. Li, W. Wu, Y. Qu and H. Tian, *J. Mater. Chem.,* 2012, **22**, 24356–24365.

27 C. Sakong, S. H. Kim, S. B. Yuk, J. Y. Kim, S. W. Park, M. J. Ko and J. P. Kim, *Bull. Korean Chem. Soc.,* 2011, **32**, 2553–2559.

28 (a) S.-H. Chan, C.-P. Chen, T.-C. Chao, C. Ting, C.-S. Lin and B.-T. Ko, *Macromolecules*, 2008, **41**, 5519–5526; (b) C.-Y. Yu, C.-P. Chen, S.-H. Chan, G.-W. Hwang and C. Ting, *Chem. Mater.* 2009, **21**, 3262–3269; (c) Y. Zhang, J. Zou, H.-L. Yip, K.-S. Chen, D. F. Zeigler, Y. Sun and A. K.-Y. Jen, *Chem. Mater.*, 2011, **23**, 2289–2291.

29 J. H. Chen, C. H. Tsai, S. A. Wang, Y. Y. Lin, T. W. Huang, S. F. Chiu, C. C. Wu and K. T. Wong, *J. Org. Chem.,* 2011, **76**, 8977–8985.

30 L. Cai, T. Moehl, S.-J. Moon, J.-D. Decoppt, R. Humphry-Baker, Z. Xue, L. Bin, S. M. Zakeeruddin and M. Grätzel, *Org. Lett.,* 2014, **16**, 106–109.

31 H. Li, T. M. Koh, Y. Hao, F. Zhou, Y. Abe, H. Su, A. Hagfeldt and A. C. Grimsdale, *ChemSusChem*, 2014, **7**, 3396–3406.

32 N. Cai, R. Li, Y. Wang, M. Zhang and P. Wang, *Energy Environ. Sci.,* 2013, **6**, 139–147.

33 N. Zhou, K. Prabakaran, B. Lee, S. H. Chang, B. Harutyunyan, P. Guo, M. R. Butler, A. Timalsina, M. J. Bedzyk, M. A. Ratner, S. Vegiraju, S. Yau, C.-G. Wu, R. P. H. Chang, A. Facchetti, M.-C. Chen and T. J. Marks, *J. Am. Chem. Soc.,* 2015, **137**, 4414–4423.

34 X. Guo, H. N. Tsao, P. Gao, D. Xia, C. An, M. K. Nazeeruddin, M. Baumgarten, M. Grätzel and K. Müllen, *RSC Adv.,* 2014, **4**, 54130–54133.

35 C.-L. Chung, C.-H. Chen, C.-H. Tsai and K.-T. Wong, *Org. Electron.*, 2015, **18**, 8–16.
36 Z. Wang, M. Liang, Y. Tan, L. Quyang, Z. Sun and S. Xue, *J. Mater. Chem. A,* 2015, **3**, 4865–4874.
37 M. Kardos, *Deutsches Reichspatent No. 276357,* **1913.**
38 C. Li and H. Wonneberger, *Adv. Mater.*, 2012, **24**, 613–636.
39 (a) S. Ferrere, A. Zaban and B. A. Gregg, *J. Phys. Chem. B*, 1997, **101**, 4490–4493; (b) S. Ferrere and B. A. Gregg, *New J. Chem.*, 2002, **26**, 1155–1160.
40 C. Zafer, M. Kus, G. Turkmen, H. Dincalp, S. Demic, B. Kuban, Y. Teoman and S. Icli, *Sol. Energy Mater. Sol. Cells*, 2007, **91**, 427–431.
41 J. Fortage, M. Severac, C. Houarner-Rassin, Y. Pellegrin, E. Blart and F. Odobel, *J. Photochem. Photobiol. A: Chem*, 2008, **197**, 156–159.
42 Y. Shibano, T. Umeyama, Y. Matano and H. Imahori, *Org. Lett.*, 2007, **9**, 1971–1974.
43 T. Edvinsson, C. Li, N. Pschirer, J. Schöneboom, F. Eickemeyer, R. Sens, G. Boschloo, A. Herrmann, K. Müllen and A. Hagfeldt, *J. Phys. Chem. C*, 2007, **111**, 15137–15140.
44 C. Li, J.-H. Yum, S.-J. Moon, A. Herrmann, F. Eickemeyer, N. G. Pschirer, P. Erk, J. Schöneboom, K. Müllen, M. Grätzel and M. K. Nazeeruddin, *ChemSusChem*, 2008, **1**, 615–618.
45 C. Li, Z. Liu, J. Schöneboom, F. Eickemeyer, N. G. Pschirer, P. Erk, A. Herrmannc and K. Müllen, *J. Mater. Chem.*, 2009, **19**, 5405–5415.
46 S. Mathew and H. Imahori, *J. Mater. Chem.*, 2011, **21**, 7166–7144.
47 A. Keerthi, Y. Liu, Q. Wang and S. Valiyaveettil, *Chem. Eur. J.*, 2012, **18**, 11669–11676.
48 (a) Z. Yao, C. Yan, M. Zhang, R. Li, Y. Cai and P. Wang, *Adv. Energy Mater.*, 2014, **4**, 1400244; (b) M. Zhang, Z. Yao, C. Yan, Y. Cai, Y. Ren, J. Zhang and P. Wang, *ACS Photonics*, 2014, **1**, 710−717.
49 (a) C. Yan, W. Ma, Y. Ren, M. Zhang and P. Wang, *ACS Appl. Mater. Interfaces*, 2015, **7**, 801−809; (b) L. Yang, Y. Ren, Z. Yao, C. Yan, W. Ma and P. Wang, *J. Phys. Chem. C*, 2015, **119**, 980−988.
50 Z. Yao, H. Wu, Y. Ren, Y. Guob and P. Wang, *Energy Environ. Sci.*, 2015, **8**, 1438−1442.
51 J. Luo, M. Xu, R. Li, K.-W. Huang, C. Jiang, Q. Qi, W. Zeng, J. Zhang, C. Chi, P. Wang and J. Wu, *J. Am. Chem. Soc.*, 2014, **136**, 265−272.
52 Q. Qi, X. Wang, L. Fan, B. Zheng, W. Zeng, J. Luo, K.-W. Huang, Q. Wang and J. Wu, *Org. Lett.*, 2015, **17**, 724−727.
53 L. Yang, Z. Zheng, Y. Li, W. Wu, H. Tian and Z. Wang, *Chem. Commun.,* 2015, **51**, 4842−4845.
54 X. Lu, T. Lan, Z. Qin, Z.-S. Wang and G. Zhou, *ACS Appl. Mater. Interfaces*, **2014**, *6*, 19308−19317.
55 X. Lu, G. Zhou, H. Wang, Q. Feng and Z.-S. Wang, *Phy. Chem. Chem. Phys.*, 2012, **14**, 4802−4809.
56 X. Wang, L. Guo, P. F. Xia, F. Zheng, M. S. Wong and Z. Zhu, *J. Mater. Chem. A,* 2013, **1**, 13328−13336.
57 Z.-S. Hunag, H.-L. Feng, X.-F. Zang, Z. Iqbal, H. Zeng, D.-B. Kuang, L. Wang, H. Meier and D. Cao, *J. Mater. Chem. A,* 2014, **2**, 15365−15376.
58 J. Shi, J. Chen, Z. Chai, H. Wang, R. Tang, K. Fan, M. Wu, H. Han, J. Qin, T. Peng, Q. Li and Z. Li, *J. Mater. Chem.,* 2012, **22**, 18830−18838.
59 Y. Wu and W. Zhu, *Chem. Soc. Rev.*, 2013, **42**, 2039−2058.
60 J.-S. Ni, J.-H. You, W.-I. Hong, W.-S. Kao, H.-H. Chou and J. T. Lin, *ACS Appl. Mater. Interfaces*, 2014, **6**, 22612−22621.
61 J.-S. Ni, W.-S. Kao, H.-J. Chou, J. T. Lin, *ChemSusChem*, 2015, DOI: 10.1002/cssc.201500193.
62 C. A. Richard, Z. Pan, H.-Y. Hsu, S. Cekli, K. S. Schanze and J. R. Reynolds, *ACS Appl. Mater. Interfaces*, 2014, **6**, 5221−5227.
63 C. A. Richard, Z. Pan, A. Parthasarathy, F. A. Arroyave, L. A. Estrada, K. S. Schanze and J. R. Reynolds, *J. Mater. Chem. A*, 2014, **2**, 9866–9874.
64 L.-P. Zhang, K.-J. Jiang, Q. Chen, G. Li and L.-M. Yang, *RSC Adv.,* 2015, **5**, 46206–46209.
65 (a) J. Zhao, T. Jin, A. Islam, E. Kwon, M. Akhtaruzzaman, N. Asao, L. Han, K. A. Alamry, S. A. Kosa, A. M. Asiri and Y. Yamamoto, *Tetrahedron,* 2014, **70**, 6211–6216; (b) J. Zhao, K. Oniwa, A. Islam, C. Qin, N. Asao, L. Han, Y. Yamamoto and T. Jin, *Org. Chem. Front.,* 2015, **2**, 253–258.
66 N. Koumura, Z.-S. Wang, S. Mori, M. Miyashita, E. Suzuki and K. Hara, *J. Am. Chem. Soc.*, 2006, **128**, 14256–14257.
67 X. H. Zhang, Z. S. Wang, Y. Cui, N. Koumura, A. Furube and K. Hara, *J. Phys. Chem. C*, 2009, **113**, 13409–13415.
68 W. Cao, M. Fang, Z. Chai, H. Xu, T. Duan, Z. Li, X. Chen, J. Qin and H. Han, *RSC Adv.*, 2015, **5**, 32967–32975.
69 A. K. Biswas, S. Barik, A. Sen, A. Das and B. Ganguly, *J. Phys. Chem. C*, 2014, **118**, 20763–20771.
70 S. Cai, G. Tian, X. Li, J. Su and H. Tian, *J. Mater. Chem. A,* 2013, **1**, 11295–11305.
71 S. Cai, X. Hu, G. Tian, H. Zhou, W. Chen, J. Huang, X. Li and J. Su, *Tetrahedron*, 2014, **70**, 8122–8128.
72 G. Tian, S. Cai, X. Li, H. Agren, Q. Wang, J. Huang and J. Su, *J. Mater. Chem. A,* 2015, **3**, 3777–3784.
73 A. Venkateswararao, P. Tyagi, K. R. J. Thomas, P.-W. Chen and K.-C. Ho, *Tetrahedron*, 2014, **70**, 6318–6327.
74 J.-Y. Su, C.-Y. Lo, C.-H. Tsai, C.-H. Chen, S.-H. Chou, S.-H. Liu, P.-T. Chou and K.-T. Wong, *Org. Lett.,* 2014, **16**, 3176–3179.
75 X. Qian, Y.-Z. Zhu, W.-Y. Chang, J. Song, B. Pan, L. Lu, H.-H. Gao and J.-Y. Zheng, *ACS Appl. Mater. Interfaces,* 2015, **7**, 9015–9022.
76 G. Ferrara, T. Jin, M. Akhtaruzzaman, A. Islam, L. Han, H. Jiang and Y. Yamamoto, *Tetrahedron Lett.,* 2012, **53**, 1946–1950.
77 (a) D. Hellwinkel and M. Melan, *Chem. Ber.*, 1974, **107**, 616–626; (b) D. Hellwinkel and M. Melan, *Chem. Ber.*, 1971, **104**, 1001–1016; (c) S. Bamberger, D. Hellwinkel and F. A. Neugebauer, *Chem. Ber.*, 1975, **108**, 2416–2421; (*d*) J. E. Field and D. Venkataraman, *Chem. Mater.*, 2002, **14**, 962–964.
78 K. Do, D. Kim, N. Cho, S. Paek, K. Song and J. Ko, *Org. Lett.*, 2012, **14**, 222–225.

Journal Name

ARTICLE

Sumit Chaurasia received his PhD degree from the Medicinal and Process Chemistry Division, CDRI, Lucknow in 2010 (under the supervision of Prof. Atul Goel). He then joined Prof. Jiann T'suen Lin's group as a postdoctoral fellow in the Institute of Chemistry, Academia Sinica. His current research interests include the design and synthesis of novel metal-free organic sensitizers for dye-sensitized solar cells.

Chia-Jung Liang received his PhD degree from the Chemistry Department of National Taiwan Normal University in 2015 (under the supervision of Prof. Ming-Chang P. Yeh). He then joined Prof. Jiann T'suen Lin's group as a postdoctoral fellow in the Institute of Chemistry, Academia Sinica. His current research interest covers the synthesis and device fabrication of metal-free organic sensitizers for dye-sensitized solar cells.

Yung-Sheng Yen obtained his Ph.D degree in chemistry from the National Taiwan University (NTU) in 2005 under the supervision of Professor Ying-Chih Lin. His recent research interests are mainly focused on the development of the functional materials for photovoltaic applications. Currently he is a assistant research scholar of the Ministry of Science and Technology in Prof. Jiann T'suen Lin's laboratory at the Institute of Chemistry, Academia Sinica, Taiwan.

Dr. Jiann T. Lin received his B.S. degree in Chemistry from the National Tsing Hua University in 1975. He completed his PhD degree in the Chemistry Department of University of Minnesota in 1984 (under supervision of Prof. John E. Ellis). After a year of postdoctoral fellow in the Chemistry Department of University of Michigan, Ann Arbor (under the supervision of Robert L. Kuczkowiki), he joined the Institute of Chemistry, Academia Sinica as an Associate Research Fellow in 1984, and was promoted to Research Fellow in 1990. He was a visiting scholar (with Prof. Tobin J. Marks) in Northwestern University in 1991. Dr. Lin is also Adjunct Professor of National Central University. His current scientific interests involve the studies of organic materials for organic light-emitting diodes, organic solar cells and two photon absorption dyes.

Table of Contents Entry

Sensitizers with Rigidified-Aromatics as the Conjugated Spacer for Dye-Sensitized Solar Cells

Sumit Chaurasia,[a]† Chia-Jung Liang,[a]† Yung-Sheng Yen,[ab]† Jiann T'suen Lin[a]*

Metal-free dyes with rigidified-aromatic segments as the conjugated spacer for dye-sensitized solar cells are compiled and reviewed.